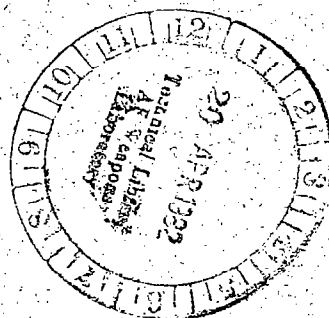TP
1985
c.1

NASA
Technical
Paper
1985

March 1982

Friction and Wear of Iron in Corrosive Media

George W. P. Rengstorff,
Kazuhisa Miyoshi,
and Donald H. Buckley

NASA

Friction and Wear
of Iron in
Corrosive Media

George W. P. Rengstorff,
Kazuhisa Miyoshi,
and Donald H. Buckley
Lewis Research Center
Cleveland, Ohio

Summary

A fundamental experimental investigation was conducted to determine the interaction of various corrosive media with iron during simple sliding friction and wear experiments. An aluminum oxide ball was made to slide across the iron surface in reciprocating motion at a relatively slow fixed speed of 9 centimeters per minute under a load of 250 grams. The corrosive media included two acids, nitric (HNO_3) and sulfuric (H_2SO_4), a salt, sodium chloride (NaCl); and a base, sodium hydroxide (NaOH) at various concentrations in water. Data for water were included for reference.

With the base NaOH at concentrations beyond 0.01 N both friction and wear decreased with an increase in normality, and X-ray photoelectron spectroscopy (XPS) surface analysis showed that this decrease was accompanied by a decrease in the surface concentration of Fe_2O_3. With the acid HNO_3 friction initially decreased with an increase in normality to 0.05 N and then remained unchanged, and XPS analysis indicates an increase in Fe_2O_3 on the iron surface. XPS analysis of those surfaces exposed to the medium H_2SO_4 revealed the presence of sulfate films on the surface in addition to Fe_2O_3. With the NaCl iron chlorides as well as oxides were present on the surface, but sodium was absent.

Introduction

Corrosion has been recognized as an important variable in the friction and wear of metals (ref. 1). Still the role of corrosion is not well understood. Most studies have been concerned with specific practical problems, such as the use of anticorrosion additives in lubricants (ref. 2) or moving parts in body implants (ref. 3). However, general basic knowledge is missing.

The effects of corrosion are complex. There is the general attack of surfaces with no particular effect in the wear contact region. However, the wear contact region differs electrochemically from the surroundings. It contains metal that is cold worked, metal that is being highly stressed elastically as well as plastically, and metal that is at locally high temperatures at shearing points (refs. 4 and 5). Electrochemical potentials can be established locally to either impede or enhance corrosion. Furthermore the high cyclic stresses may promote stress corrosion and corrosion fatigue (ref. 6).

Resistance to corrosion is often the result of the formation of some type of a film on the metal surface. Wear can destroy such films. Alternatively, wear could develop better corrosion-resistant films by producing new surfaces. Furthermore the coefficient of friction is, like corrosion resistance, highly sensitive to surface films.

The study reported herein is the start of a systematic investigation of the role of corrosion in the friction and wear of metals. Experimentally a loaded spherical aluminum oxide rider was made to slide, while in various solutions, on the flat surface of iron in reciprocal motion. The solutions studied were (1) NaOH between 0.0001 N and 20 N, (2) HNO_3 between 0.0005 N and 1.0 N, (3) H_2SO_4 between 0.0001 N and 35.6 N, and (4) NaCl between 0.0001 N and 1.0 N. As a reference, similar experiments were made in water.

The load on the rider was 250 grams. The iron flat was moved for a distance of 1 centimeter under the rider in reciprocal motion. The duration of each experiment was 1 hour, during which the rider passed over the center section of the track 540 times.

Static coefficients of friction were measured throughout the experiments. The kinetic coefficient of friction was established for conditions where stick-slip was important. Photomicrographs were obtained of each specimen. Selected conditions were repeated on differently mounted specimens for analysis by SEM (scanning electron microscopy) and by XPS (X-ray photoelectron spectroscopy). All specimens, except this latter group, were scanned across the track by a surface profilometer to determine the profile of the track and its width.

Materials

The iron used in these studies was better than 99.99 percent pure and was fully annealed. The water used in the experiments and in making solutions was deionized, distilled, and vacuum degassed. The NaOH used in making solutions was in the form of certified American Chemical Society (ACS) electrolytic pellets. The HNO_3 was ACS reagent-grade concentrated acid (i.e., 15.4 N, or 69 percent HNO_3). The H_2SO_4 also was ACS reagent-grade concentrated acid (i.e., 35.6 N, or 95 percent H_2SO_4). The NaCl was in the form of crystals.

Apparatus

The apparatus used in this investigation is shown schematically in figure 1. The rider was an aluminum oxide (sapphire) ball, 6 millimeters in diameter, mounted in a holder.

Most of the specimens were irregularly shaped pieces of iron mounted with an epoxy cement onto a fiberglass–plastic holder. The holder was held by a vise in a jig that was moved reciprocally under the rider. The holder kept the solution that spilled off the top of the specimen surface from flowing into the unit and with a shield prevented the solution from spattering during a run.
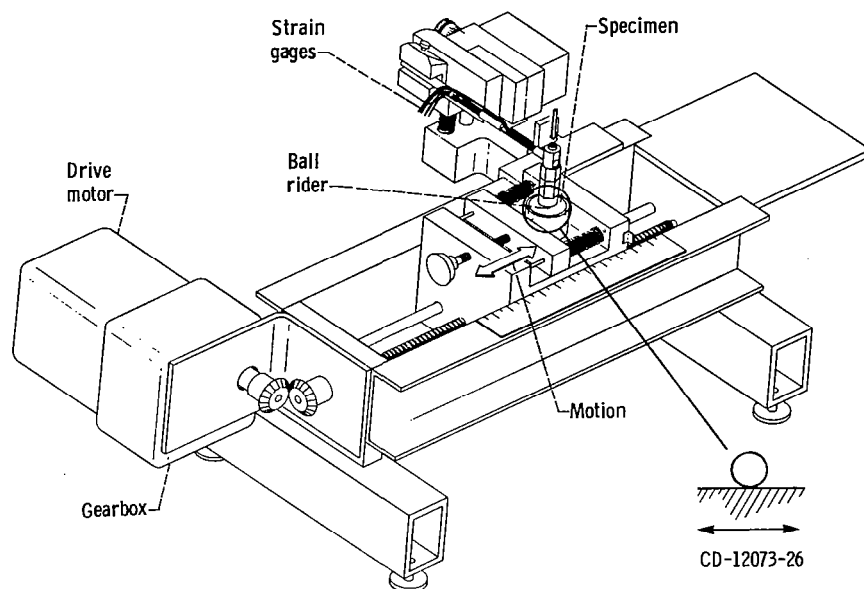
Figure 1. - Friction and wear apparatus.

Since these specimens could not be used in the high-vacuum system of the SEM and XPS, short stainless-steel cylinders (10 mm diam), which fit into the holders for the SEM and XPS units, formed the base. Flattened and annealed high-purity iron rods were attached to the end of each stainless-steel cylinder with an epoxy developed for use in high vacuum. A wire was then spot welded to the side of the specimen and to the cylinder for electrical continuity.

As indicated in figure 1, the mounted iron specimens held in the jig were moved back and forth under the loaded rider. The motion of the specimen was 10 millimeters in each direction, but the tracks were shorter: The track length varied somewhat because of the friction at the end of each reversal. The rider carried a load of 250 grams. The arm holding the rider was flexible so that the friction force F could be measured with the aid of calibrated strain gages and continuously recorded.

There were nine reversals per minute (i.e., the flat specimen traveled at an average speed of 9 cm/min), and each experiment lasted 60 minutes. Thus the rider passed over the center section of the track 540 times (270 times each way) during the course of an experiment. It was the center section that was studied in this work.

The apparatus was housed in a plastic box in which a positive pressure of argon gas was maintained.

Experimental Procedure

The iron flats were metallographically ground with 600-grit paper and then polished with diamond paste: first 6-micrometer paste, then 3-micrometer paste. Final polishing was with 0.3-micrometer alpha alumina on a flooded, flat polishing wheel. The polished specimen was cleaned with a strong flow of tap water and dried with ethanol. The dried specimen was etched with 5 percent nital until the disturbed metal was removed and the grain structure was visible. Then the specimen was lightly polished with the 0.3-micrometer alumina, washed with a strong flow of tap water, dried with ethanol, and cleaned ultrasonically in Freon for ½ hour to dislodge any clinging alumina. The specimens were again washed with ethanol and dried.

In the individual experiments the mounted specimens were clamped into the jig in the box. The rider was lowered to about 4 millimeters above the surface of the iron. Several drops of the desired solution were squirted under the rider and on the surface near the rider to form one large drop covering most of the surface of the iron specimen. The rider was lowered through the drop until a strain gage showed that it just touched the iron surface. When this was accomplished, the 250-gram weight was loaded onto the rider, the box was closed, and the argon purge begun. Then sliding was initiated and continued for 1 hour.

The drop of liquid immediately formed a meniscus between the rider holder and the iron surface and remained there during the course of each experiment. Thus the rider and its point of contact with the iron were always in the interior of a large liquid drop. Furthermore the meniscus provided a continuous supply of solution to keep the rest of the iron wet in and near the wear track.

The friction force of the rider moving across the iron in the wear track was determined by strain gages on the flexible arm that held the loaded rider. The output from the calibrated strain gages was recorded continuously. The coefficient of friction then was the force divided by the load on the rider (250 g). The static coefficient μ_s was the maximum F in each direction of travel or, as used, half the maximum force in a complete reversal of travel. The kinetic coefficient was estimated in the usual manner by using the force as the mean between the maximum force (stick) and the minimum force (slip) when stick-slip

2

occurred (ref. 5). It is the mean between the maximum and minimum because momentum carries the rider an equal distance past the force for μ_S when it starts moving from the "stick" position.

XPS Procedure

X-ray photoelectron spectroscopy (XPS) was used to analyze wear surfaces generated during the friction and wear experiments in the various media. Details of the XPS system used and the procedure followed can be found in reference 6.

To obtain reproducible results, a strict standardization of the order and time of recording was used. The instrument was regularly calibrated. The analyzer work function was determined by assuming the binding energy for the gold 4f 7/2 peak to be 83.8 electron volts. That is, the gold 4f 7/2 peak was used as the reference line. All survey spectra (scans of 1050 or 1100 eV) were taken at a pass energy of 50 or 100 electron volts, and this provided the instrumentation resolution of 1 electron volt at room temperature. The magnesium Kα X-ray was used with an X-ray source power of 400 watts (10 kV, 40 mA). The narrow scans of the carbon 1s, silicon 2p, and oxygen 1s peaks were just wide enough to encompass the peaks of interest and were obtained with a pass energy of 25 electron volts at room temperature.

To evaluate the charging effect and to determine accurately the energy and shape of peaks, spectra were recorded several times. Resolution of the spectral peak is 1.56 electron volts full width. The energy resolution is 2 percent of the pass energy, that is, 0.5 electron volt. The peak maximums can be located to ±0.1 electron volt. The reproducibility of peak height was good, and the probability of error in the peak heights ranged from ±2 percent to ±8 percent. Peak ratios were generally good to ±10 percent or less.

(a) Photomicrograph of wear track.

(b) SEM photograph of edge of wear track made with secondary-electron mode. (Wear track is at top of photograph.)

Figure 2. - Wear track on iron surface, generated in water.
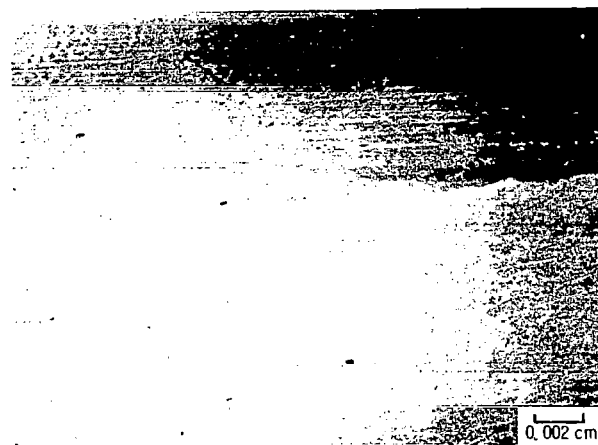
Results and Discussion

Water

As a basis on which to compare the effects of various solutions, experiments were conducted initially with water as the corrosive medium. The μ_S for each of the three experiments was fairly reproducible, with values of 0.26, 0.29, and 0.30 being obtained. The friction coefficients for water can be classified as "moderate." Many solutions gave lower values; a few gave higher values.

A photomicrograph and an SEM photograph of the wear of one of the experiments in water are shown in figure 2. It is interesting to note that the wear tracks obtained in water were easily seen in the light microscope and difficult to observe with the SEM. The SEM shows the track to be smooth. The ease of observation with reflected light probably results from the formation of a thin, dark surface oxide that provides contrast. If this conclusion is correct, water can be considered as corrosive under these conditions. The formation of the film could come from oxygen in the water, even though it had been purified and degassed. On the other hand, direct oxidation by water (steam) could have taken place at the local hot spots where shear occurs during wear.

The top curve in figure 3 shows the profile of the specimen wear track obtained in water. A considerable amount of metal has been moved around to form a sharp lip at the edges of the wear track.

Sodium Hydroxide

The variation of the static coefficient of friction (μ_S) with NaOH concentration is presented in figure 4, and a comparable variation in the kinetic coefficient of friction μ_k in figure 5. In this NaOH system there is a clear maximum in μ_S at 0.01 N. All three experiments at 0.01 N show μ_S between 0.46 and 0.52. Not only were the final results consistent, but the μ_S during the course of each experiment was consistently high. At a lower
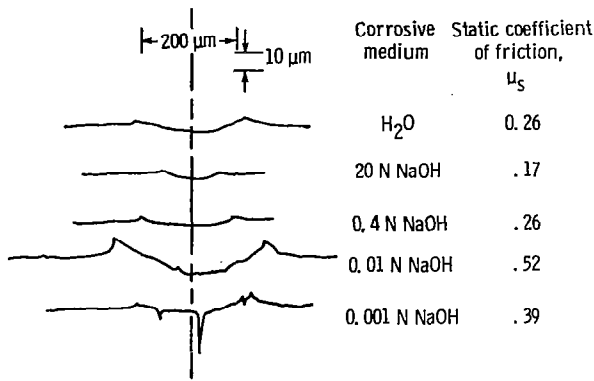
Figure 3. - Talysurf traverses across wear tracks generated by Al_2O_3 ball sliding on iron flat in various media. (Wear tracks were made on the iron flat.)
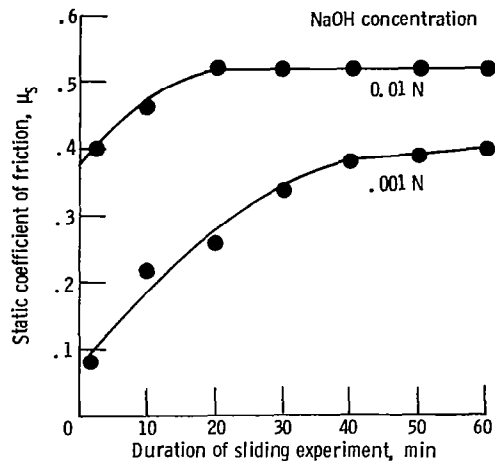

Figure 6. - Typical change of static coefficient of friction with time for Al_2O_3 ball sliding on iron flat in 0.01 N NaOH and 0.001 N NaOH solutions.
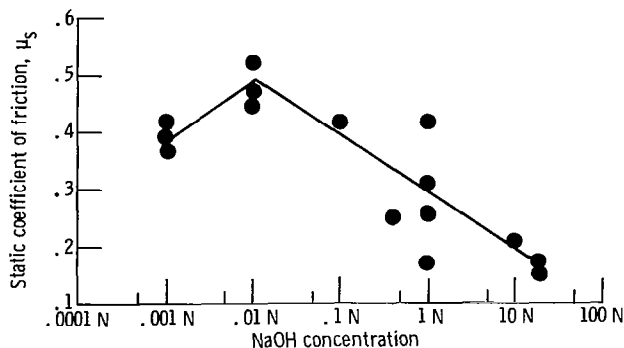

Figure 4. - Effect of NaOH concentration on static coefficient of friction for Al_2O_3 ball sliding on iron flat in NaOH solutions.
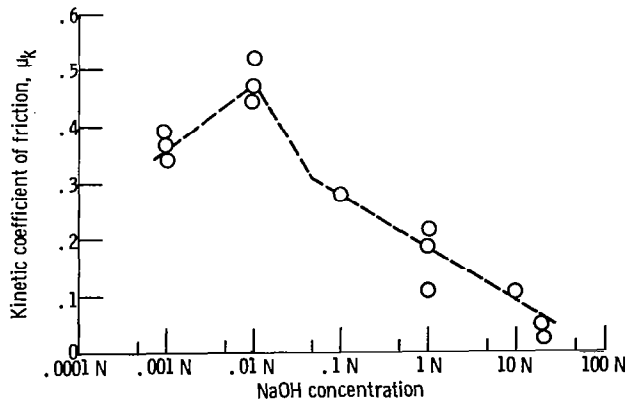

Figure 5. - Effect of NaOH concentration on kinetic coefficient of friction for Al_2O_3 ball sliding on iron flat in NaOH solutions.

concentration (0.001 N), although the final μ_s was only a little lower, the time-dependent behavior was very different. Time-dependent μ_s curves for a 0.001 N and a 0.01 N experiment are compared in figure 6. At concentrations of NaOH higher than 0.01 N, the μ_s continuously dropped to around 0.02 and below as NaOH increased to 10 N or above. However, there is a large scatter around a fairly distinct line in μ_s between 0.04 and 1.0 N (fig. 4). The reason is not clear.

The curve for μ_k against NaOH concentration (fig. 5) is generally parallel to the curve for μ_s. However, at 0.01 N NaOH, where μ_s was highest, there was no stick-slip.

From the standpoint of corrosion alone, it must be realized that steel, and presumably thus iron, is not attacked overall by any concentration of NaOH. Still, NaOH is famous for causing "caustic embrittlement" of steel. This problem has been known for over 100 years as a major cause of explosions in railroad and stationary boilers (refs. 7 to 9).

It is now known that caustic embrittlement is a classic case of stress corrosion failure (ref. 8). Overall corrosive attack is low. However, in regions under elastic strain, pitting and grain boundary attack occur. These progress by some mechanism and with applied or residual stresses lead to brittle fracture in accordance with the principles of fracture mechanics.

The iron in the track is certainly under a high local elastic stress when the rider passes over. It retains high residual elastic stresses because of local plastic deformation. This might be an area where the pitting and grain boundary attack inherent in caustic embrittlement start. This was observed with 0.001 N NaOH. A region of the track showing grain boundary attack is presented in figure 7(a), and a surface profile trace across one of the pits in another region of the same wear track in figure 7(b). Figure 3 shows a surface profile scan across several wear tracks made after various experiments. The lowest trace in figure 3 shows that a deep pit does indeed
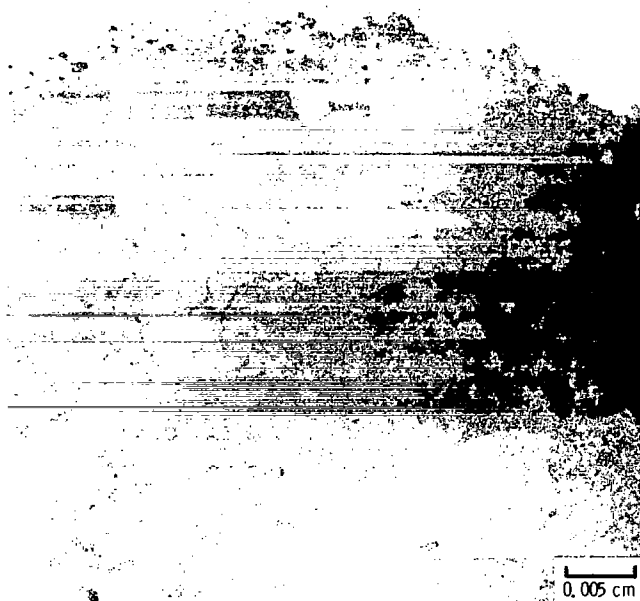
(a) Region of wear track showing grain boundary attack.
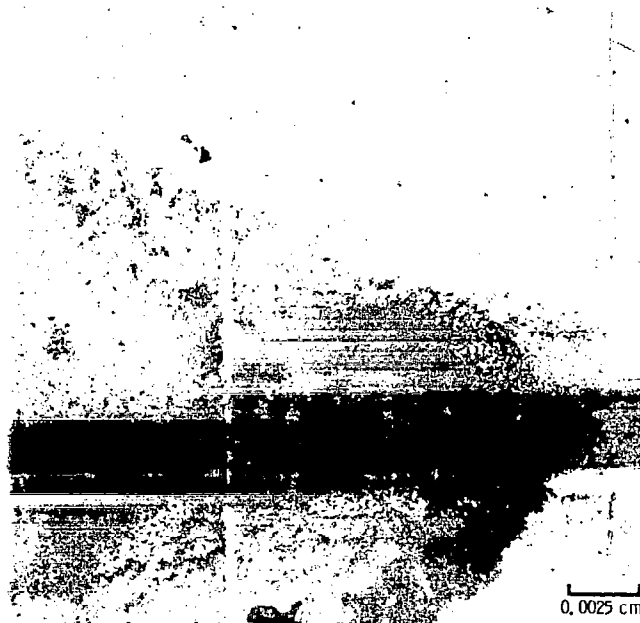
(b) Talysurf track across wear track through pit in pitted region.

Figure 7. – Photomicrographs of wear track generated by Al_2O_3 ball sliding on iron flat in 0.001 N NaOH solution.

exist where it appears to exist in the photomicrograph of figure 7(b).

A similar specimen from the 0.001 N NaOH experiment was made for the SEM study. A photomicrograph of the wear track of this specimen is shown in figure 8(a). There was some problem in obtaining a clear picture because of the variable depth of the track. Nevertheless the structure at the bottom of the track indicates chemical attack. Actually most of the grains in the iron are fine enough to suggest that the structure comes from partial grain boundary attack.

A section across the complete track at twice the magnification is shown in figure 8(b). This is possible because of the considerable depth of focus of the SEM. It appears that a film at least partially developed but broke down under the repeated sliding of the rider over the surface. Pits formed, as well as elongated faults that appear to be associated with underlying grain boundaries of the iron.

The usual mode of operating the SEM is to use secondary electrons, as in figure 8(b). It is probable that the bright outlines of pits and other defects are caused by foreign ions strongly emitting. The true contour of the surface is brought out more clearly with the backscattering mode of operation, as is shown in figure 8(c) for the same region at the same magnification as that presented in figure 8(b).

The defect in the centers of figures 8(b) and (c) is shown at much higher magnification in figure 8(d). It is clear that a difference in level exists along a sharp line for the different parts of this defect. The dark (higher or lower) section is too small to be a single grain. It may be associated with part of an iron grain and its boundary. It may also be a broken section of a surface film.

Figure 9 shows a photomicrograph and SEM photographs of the wear track made in the 0.01 N NaOH solution, which consistently gave the highest friction, ($\mu_s = 0.47$). The photomicrograph (fig. 9(a)) shows a track that is highly disturbed. The surface profile track of a duplicate specimen shown in figure 3 (second curve from bottom) reveals that the center of the track was rough. Still, there was no evidence of deep pits and/or deep grain boundary attack as with some of the specimens generated in 0.001 N NaOH, as discussed previously. On the other hand the SEM photograph shows shallow pits, linear upheavals, and other disturbances in the center of the wear track made in 0.01 N NaOH that are even more severe than those produced in the lower concentration medium.

A noteworthy point is that the entire width of the wear track appeared, under reflected light in the microscope, to be about equally disturbed. The SEM shows that the center third but not the entire track, had a structure that can be described as highly broken. On each side of this center section is a broad region that appears smooth, except for small pits in some localities.

Comparison of the SEM photographs taken with the secondary-electron and backscattering modes strongly suggests that a highly ionizing foreign material is active in the formation of the disturbed structure that is associated with high friction. It is again suggested that a low-friction film tends to form but is broken down under the conditions encountered in these experiments. This exposes high-friction material (iron) from below the film. Furthermore it is suggested that this surface film
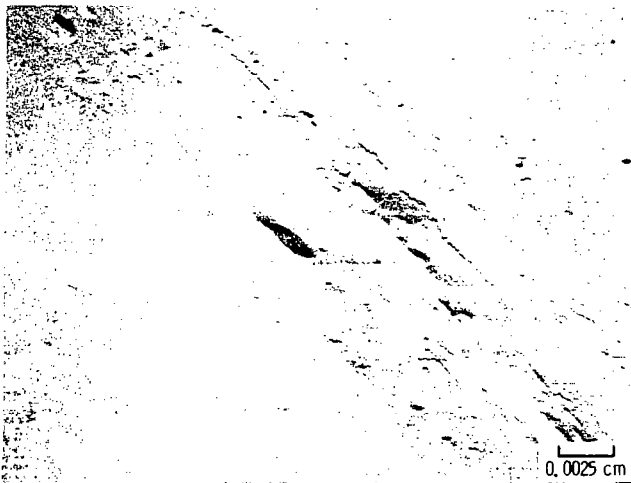
5

(a) Photomicrograph of wear track

0. 005 cm

(b) SEM photograph of wear track, made with secondary-electron mode.

0. 0025 cm

0. 0025 cm

(c) SEM photograph of wear track, made with backscattering mode.

0. 0002 cm

(d) SEM photograph of defect in center of (b) and (c), made with secondary-electron mode.

Figure 8. - Photomicrographs of wear track generated by Al_2O_3 ball sliding on iron flat in 0. 001 N NaOH solution.

breakdown is related to the elastic stress conditions that cause the pitting and grain boundary attack characteristic of NaOH stress corrosion of plain carbon steel.

The high-friction wear tracks in NaOH discussed previously can be compared with low-friction wear tracks also obtained in NaOH solutions. A concentrated solution, 20 N, gave a μ_s of 0.17. Figure 10 shows a photomicrograph and SEM photograph of a specimen obtained in one of these experiments. Note how smooth the wear track appears, even at the highest magnification. The small amount of metal disturbed at this low friction is shown in the second profile in figure 3. Surely, under these conditions, a tenacious film forms that does not break up, and this film acts as a lubricant. That the amount of metal disturbed in the wear track is directly proportional to the μ_s when operating in NaOH is shown in figure 11.

Nitric Acid

The effect of HNO_3 on the coefficient of friction is shown in figure 12. In the concentration range 0.005 N HNO_3 to 1.0 N HNO_3 (the maximum studied), the value of μ_s was constant at about 0.23. This is a little lower than the value observed for water. This independence of coefficient of friction over a wide concentration range is somewhat surprising in this system. Plain carbon steel is not recommended for service in HNO_3 at any concentration because of the rate of general attack and the inconsistency of the formation of passivating films (ref. 7).

Over the range where μ_s was constant, general corrosion varied greatly and the appearance of the wear track also varied. This is illustrated by the photomicrographs in figure 13. As shown in figure 13(a)

(a) Photomicrograph of wear track.

(b) SEM photograph of wear track, made with secondary-electron mode.

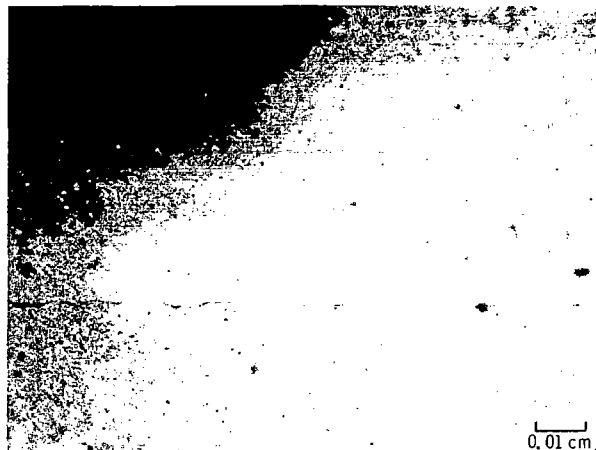(c) SEM photograph of same area as (b), made with backscattering mode.

(d) SEM photograph of center of wear track, made with secondary-electron mode at higher magnification than (b).

(e) SEM photograph of same area as (d), made with backscattering mode.

Figure 9. - Photomicrograph of wear track generated by Al_2O_3 ball sliding on iron flat in 0.01 N NaOH solution. Static coefficient of friction, μ_s, 0.47.
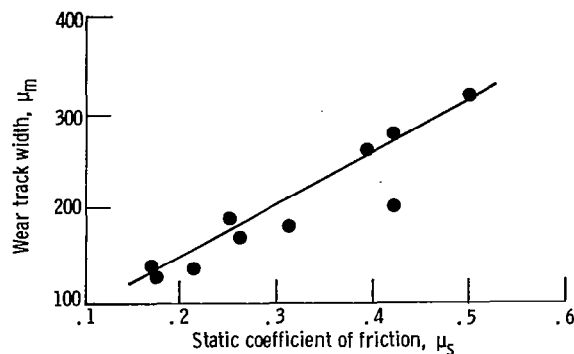
(a) Photomicrograph of wear track.

0.01 cm

0.0025 cm

(b) SEM photograph of wear track, made with backscattering mode.

0.00007 cm

(c) SEM photograph of center of track made with secondary-electron mode at higher magnification.

Figure 10. - Photomicrographs of wear track generated by Al_2O_3 ball sliding on iron flat in 20 N NaOH solution. Static coefficient of friction, μ_s, 0.17.

Figure 11. - Relation between wear track width and static coefficient of friction for Al_2O_3 ball sliding on iron flat in NaOH solutions.
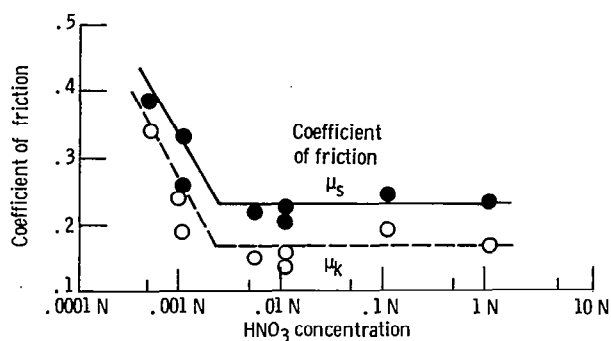

Figure 12. - Effect of HNO_3 concentration on coefficient of friction for Al_2O_3 ball sliding on iron flat in HNO_3 solutions.

general corrosion was severe at 1.0 N HNO_3. It cut into the wear track to give a very irregular pattern. At 0.1 N HNO_3 there was deep grain boundary etching outside the wear track, as shown in figure 13(b). At 0.01 N HNO_3 general pitting occurred outside the wear track, as shown in figure 13(c).

Figure 14 shows that a relation exists between μ_s and width of the wear track in HNO_3 just as it did in NaOH.

Sulphuric Acid

The effect of H_2SO_4 concentration on the coefficients of friction is shown in figure 15. At first observation it appears that the coefficients of friction, both μ_s and μ_k, were independent of concentration from the very dilute 0.0001 N to the very concentrated 35.6 N. There could have been a slight increase at the dilute end, but this is questionable.

To get a better understanding of what was happening in the wear track formed in H_2SO_4, a specimen operated in 0.01 N H_2SO_4 was selected for an SEM study. The photomicrograph in figure 16(a) shows that there was considerable general corrosion outside the wear track in 0.01 N H_2SO_4. The SEM photograph in figure 16(b) showing the entire width of the track suggests that the track surface was highly roughened. The SEM photograph taken with the backscattering mode
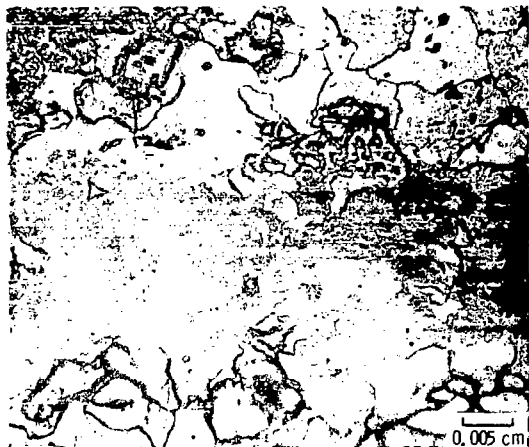
(a) 1. 0 N HNO₃.

(b) 0. 1 N HNO₃.
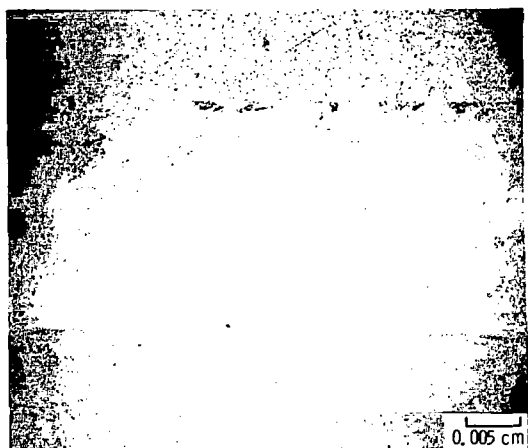
(c) 0. 01 N HNO₃.

Figure 13. - Photomicrographs showing variations in appearance of wear track and general corrosion for Al₂O₃ ball sliding on iron flat in various concentrations of HNO₃.
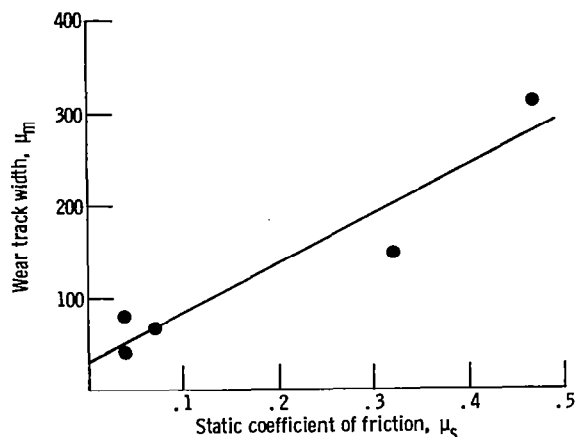

Figure 14. - Relationship between wear track width and static coefficient of friction for Al₂O₃ ball sliding on iron flat in HNO₃ solutions.
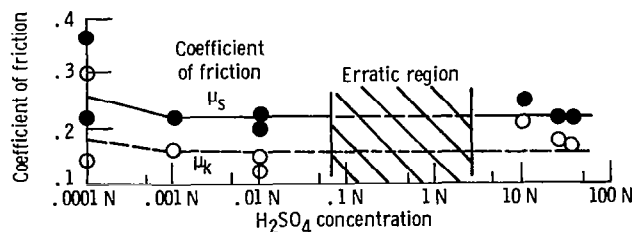

Figure 15. - Effect of H₂SO₄ concentration on coefficient of friction for Al₂O₃ ball sliding on iron flat in H₂SO₄ solutions.

(fig. 16(c)) shows that there was some roughness of the track surface but that a good deal of the structure in figure 16(b) came from strong electron-emitting regions presumably associated with foreign ions. Figure 16(c) does show that the lip at the edge of the track was corroded a great deal more than the track itself. Figure 16(d) shows in greater detail the extent of the pitting and roughening in the track.

Sulfuric acid is strongly passivating to iron under some conditions. In fact, at concentrations above about 76 to 80 percent, steel corrodes slowly enough so that plain carbon steel is recommended for containers and other service with H_2SO_4 (ref. 7). This slow reaction is due to the formation of a passivating film. Steel is not recommended for use with H_2SO_4 at lower concentrations.

It was thought that if concentrated acid markedly slowed corrosion by film formation, it might also change the coefficient of friction. It did not. Concentrations of 70 percent H_2SO_4 (26.2 N) and 95 percent H_2SO_4 (35.6 N) gave the same coefficient of friction as lower concentrations ($\mu_s = 0.22$).

For H_2SO_4 there was no consistent relation between μ_s and track width. This was partly due to the small range in values of μ_s. It should be noted, however, that at 10 N and above the track widths were greater than justified by μ_s. It appears that corrosion in the track was adding to
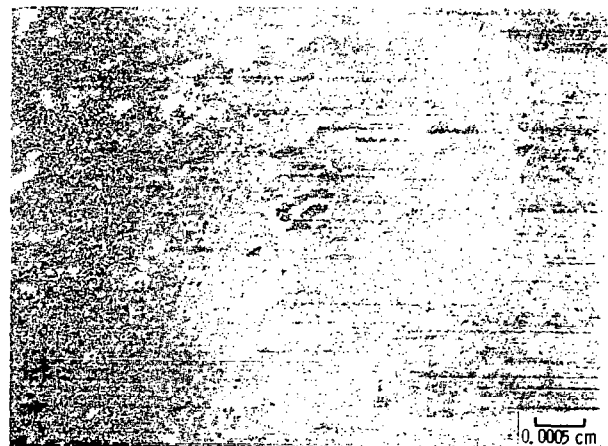
(a) Photomicrograph of wear track.

(b) SEM photograph of wear track, made with secondary-electron mode.

(c) SEM photograph of same area as (b), made with backscattering mode.

(d) SEM photograph of center of wear track, made with secondary-electron mode at higher magnification than (b).

Figure 16. - Photomicrographs of wear track generated by Al_2O_3 ball sliding on iron flat in 0.01 N H_2SO_4 solution.

metal deformation and/or removal. This effect was not observed for any concentration of HNO_3, NaOH, or NaCl.

Sodium Chloride

The results of experiments with NaCl solutions are summarized in table I, and the relation between NaCl concentration and coefficient of friction is shown in figure 17.

In fact, there was little, if any, change between the very dilute 0.0001 N NaCl and 1.0 N NaCl. A slight drift downward from a μ_s of 0.29 at 0.0001 N typical of distilled water down to a μ_s of 0.23 at 1.0 N is too small a change to be significant. However, it should not be concluded on the basis of these experiments that salt in the water is of no importance. It is well understood that NaCl does not play a direct part directly in the corrosion of iron (ref. 7). Its principal effect is in making water electrically conductive so that oxygen in the water can cause corrosion. It can also operate indirectly to cause

TABLE I. – EXPERIMENTAL
RESULTS IN
SODIUM CHLORIDE MEDIUM

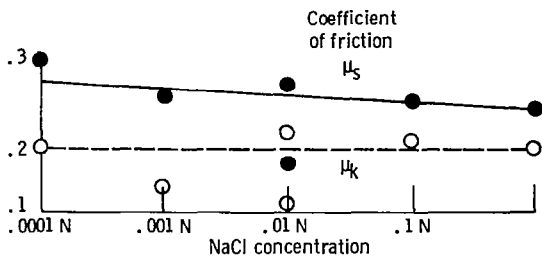| Normality of NaCl in H_2O	Static coefficient of friction, μ_s	Track width, μm
Water	0.28	220
0.0001 N	.29	200
0.0005 N	.29	200
0.001 N	.25	180
0.005 N	.25	180
0.01 N	.21	150
0.1 N	.24	190
0.4 N	.24	190
1.0 N	.23	130

Figure 17. - Effect of NaCl concentration on coefficient of friction for Al$_2$O$_3$ ball sliding on iron flat in NaCl solutions.

HCl to build up locally at pits, crevices, etc., and it has some other complex indirect effects.

A study of the effect of NaCl should be accompanied by a variation of oxygen content. The 1.0 N NaCl solution used herein was found to contain 6.5 ppm oxygen. This is of the order of one-fourth the maximum oxygen content of room-temperature water in contact with air. This was the solution used to prepare the more dilute solutions. As discussed earlier it was made with distilled, vacuum-degassed water. However, when working with NaCl solutions, it would be well to degas some solutions just before the friction experiments and to saturate others with oxygen in order to get a qualitative picture of the effect of oxygen in NaCl.

The pH of the salt solution might also be important. The 1.0 N solution was found to have a pH of 6.35; this is nearly neutral but slightly on the acid side.

An SEM study was made of a friction specimen prepared in a 0.01 N NaCl solution. It had a μ_s of 0.26, similar to the μ_s of most of the other specimens run in NaCl solutions. Figure 18(a) shows the photomicrograph of this specimen. It appears to be roughened all across the wear track but particularly on one side. The SEM photograph of the entire track (fig. 18(b)), taken with the secondary-electron mode, shows the track to be much darker than the areas outside the track. In fact, it looks very much like the track obtained with 0.01 HNO$_3$. Higher magnification with the SEM using the secondary-electron mode (fig. 18(c)) shows mainly striations similar (but not identical) to those observed with water (fig. 2(b)). However, there is a darker "ghost pattern" crossing the striations. This pattern appears to be the darker structure in figure 18(b) and in the photomicrograph (fig. 18(a)). Because the backscattering mode did not show much but a smooth surface, it is not included here.

The wear surfaces of iron under equivalent concentrations (0.01 N) of nitric and sulfuric acids, sodium chloride, and sodium hydroxide in water were examined with XPS. The results obtained are presented in figure 19. Data for water as the solvent are included for reference.
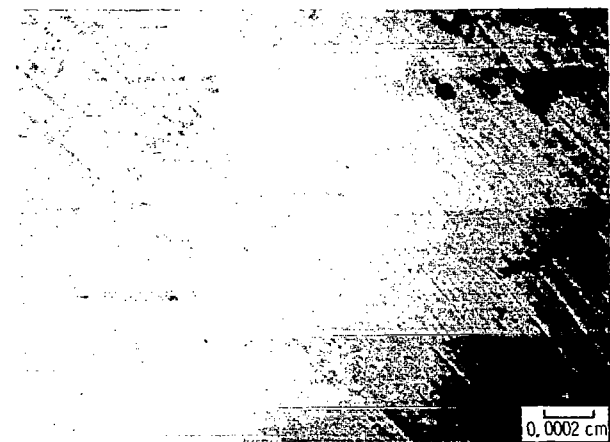
In figure 19(a) Fe$_2$O$_3$ is seen in all the spectra; the oxygen 1s peak for Fe$_2$O$_3$ occurs at 530 eV. The peak intensity varies with the medium. Beginning with nitric acid it decreases as HNO$_3$ > H$_2$SO$_4$ > NaCl > NaOH, with H$_2$O falling between the two acids HNO$_3$ and H$_2$SO$_4$.
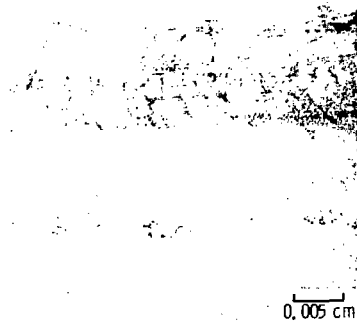
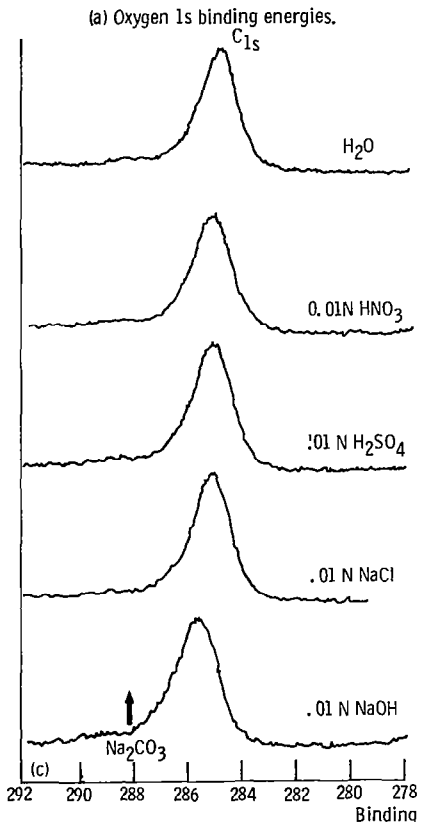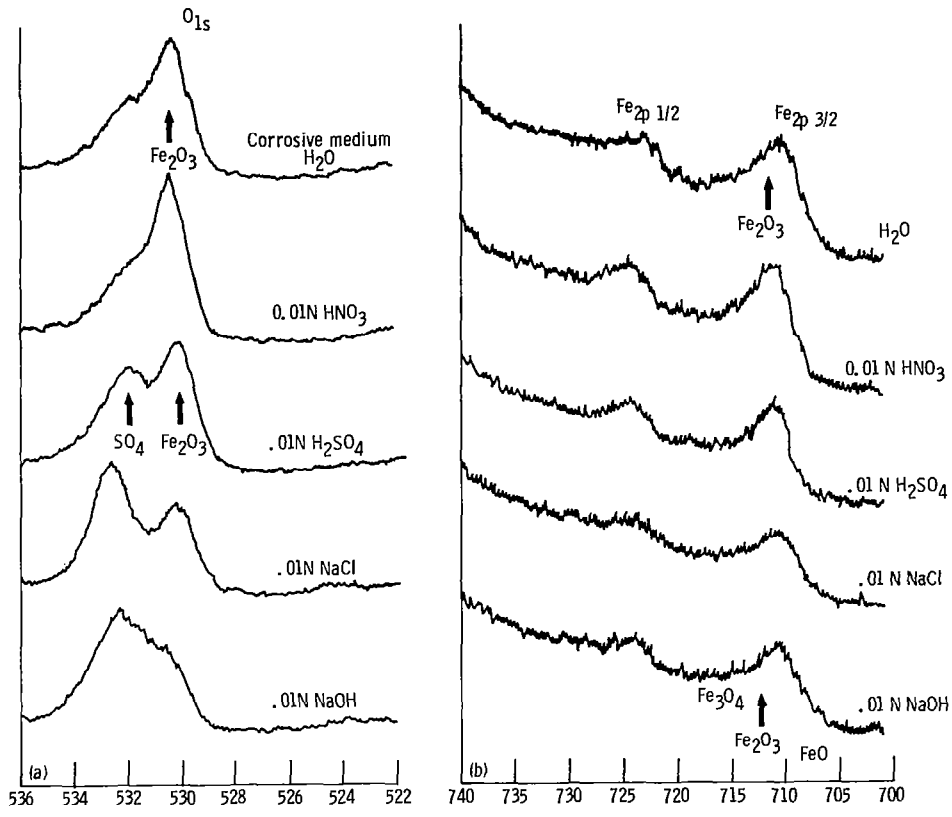(a) Photomicrograph of wear track.

(b) SEM photograph of wear track, made with secondary-electron mode.

(c) SEM photograph of interior of wear track, made with secondary-electron mode.

Figure 18. - Photomicrographs of wear track generated by Al$_2$O$_3$ ball sliding on iron flat in 0.01 N NaCl solution. Static coefficient of friction, μ_s, 0.26.

(a) Oxygen 1s binding energies.

(b) Iron 2p 3/2 binding energies – 740 to 700 eV.

(c) Iron 2p 3/2 binding energy – 716 to 702 eV.

(d) Carbon 1s binding energies.

Binding energy, eV

Figure 19. – XPS data on wear surface of iron.

12

Ferric oxide is abrasive. However, the wear of iron in water, HNO_3, and H_2SO_4 decreases with an increase in Fe_2O_3 peak intensity. A sulfate $(SO_4)O$ is present on the wear surface under H_2SO_4. The interesting observation to be made from figure 19(a) is that the spectra vary with the medium.

The data of figures 19(b) and (c) for the iron 2p 3/2 binding energies again indicate that Fe_2O_3 is present in all spectra. There is little question but that Fe_2O_3 forms in all media, varying only in the quantity formed on the surface with rubbing.

The carbon 1s data of figure 19(d) do not indicate much in the way of variations in peak intensity. Likewise the origin of the carbon appears consistent.

Analyses of the key elements present in the acids HNO_3 and H_2SO_4, the salt NaCl, and the base NaOH were made with XPS. The results are presented in figure 20. Figure 20(a) shows the presence of nitrogen from the HNO_3 medium. The nitrogen 1s peak occurred at a binding energy of 397.9 electron volts.
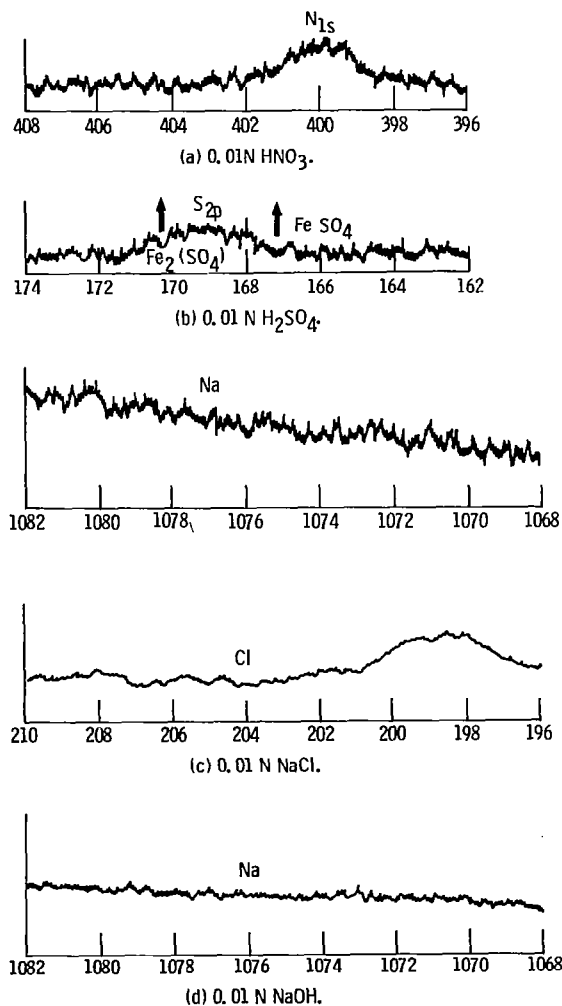
Analysis of the iron surface rubbed under 0.01 N H_2SO_4 (fig. 20(b)) showed a sulfur peak at 169 electron volts of binding energy. The sulfur 2p peak is associated with the surface compounds $Fe_2(SO_4)_3$ and Fe_2O_3, a likely surface candidate compound resulting from the chemical variation of H_2SO_4 with iron in an aqueous environment. The peak can be seen in the spectrum of figure 20(b).

XPS spectra obtained from the iron wear surface generated in 0.01 N NaCl (fig. 20(c)) are interesting in that the sodium spectrum fails to indicate the presence of any sodium on the iron surface. The lower spectrum of figure 20(c), that for chlorine, does reveal the presence of chloride. The binding energy of figure 20(c) at 199 electron volts matches that for both $FeCl_2$ and $FeCl_3$, which are extremely close in energies and difficult to distinguish in the data of figure 20(d).

With NaOH as the surface medium, sodium was absent on the wear surface, as indicated in the spectrum of figure 20(d). This absence of sodium is similar to what was observed with NaCl.

The chemistry of the surface films varied not only with the different media placed on the surface, but also with changes in the concentration of a single fluid. For example, simply changing the normality of the NaOH solution resulted in a different surface chemistry on the wear surface, as indicated in the data of figure 21.
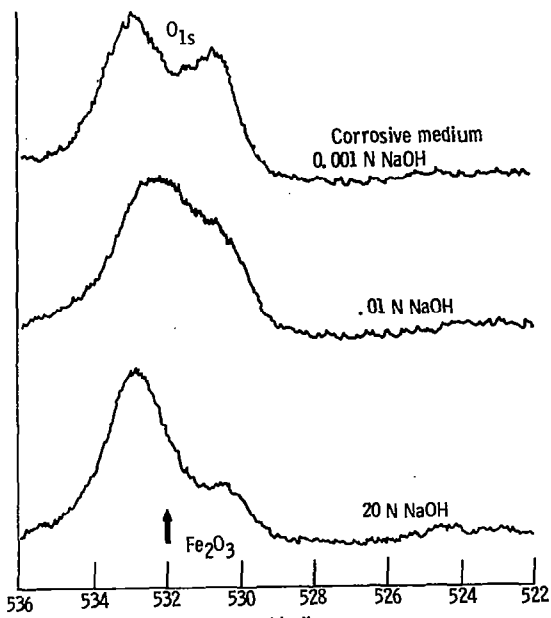
In figure 21(a) the oxygen 1s peak associated with Fe_2O_3 is observed to decrease in intensity with an increase in NaOH concentration. The static friction coefficient decreased with increasing NaOH normality in this concentration range in figure 2, and wear was minimal with the 20 N NaOH in figure 6. Thus, with NaOH, a base, a decreasing surface concentration of Fe_2O_3 is brought about by an increase in NaOH normality, and this results in a decrease in both friction and wear.

The iron 2p 3/2 binding energies in figures 21(b) and (c) confirm the Fe_2O_3 observation. The spectra of figure 21(d) indicate an absence of sodium in the wear region at all three concentrations.
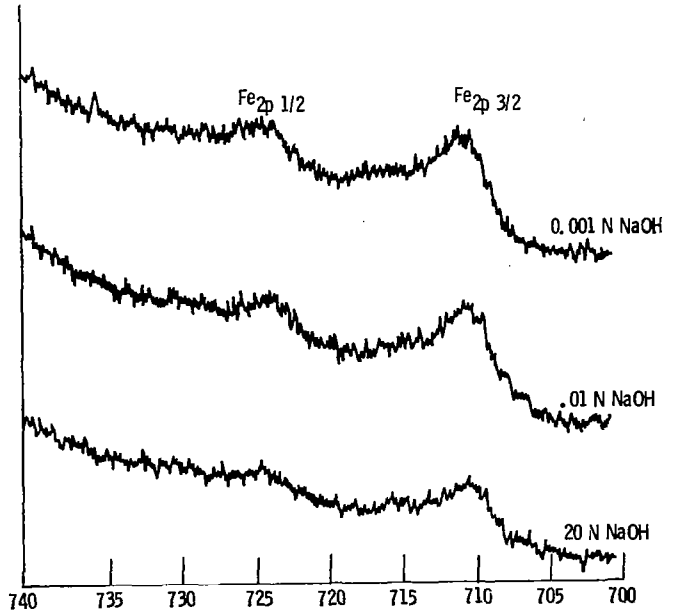
Just as variations in concentration of the base NaOH produced different surface films, similar observations were made for the acids. For example, an increase in the normality of HNO_3 on the iron surface resulted in an actual surface film. Increasing the normality of HNO_3 from 0.001 N to 0.01 N resulted in an increase in the amount of Fe_2O_3 on the iron surface, as indicated in the XPS data of figure 22. However, with NaOH an increase in concentration resulted in a decrease in the amount of Fe_2O_3 present on the surface. Thus, while increasing the concentration of the acid HNO_3 increased the amount of Fe_2O_3 found on the surface, increasing the concentration of the base NaOH had the opposite effect.

Figure 20. - XPS elemental analysis of iron wear scars in various media.
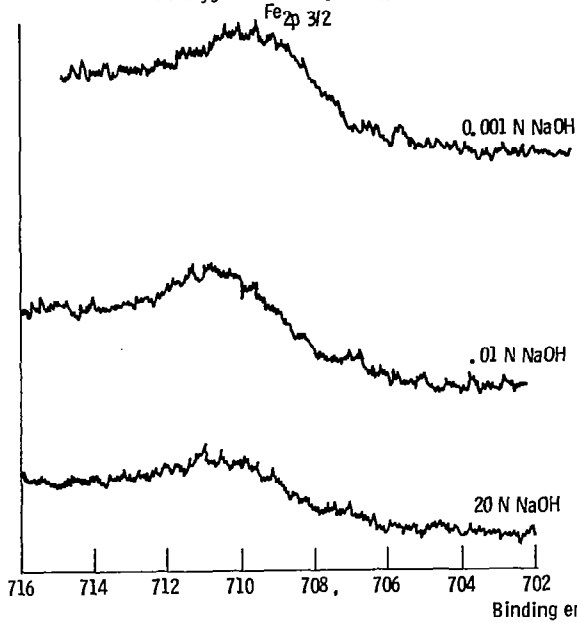
Conclusions

Based on the experimental results obtained in this investigation, with iron examined in corrosive media in various concentrations, the following conclusions were drawn:
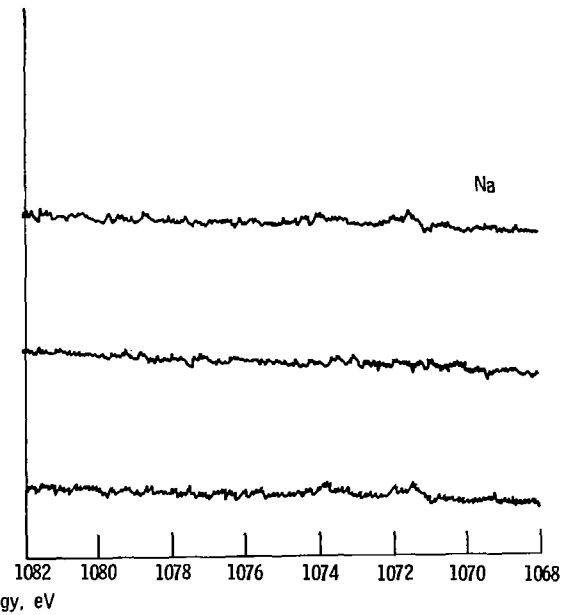
O_{1s}

Corrosive medium
0.001 N NaOH

.01 N NaOH

20 N NaOH

Fe_2O_3

536   534   532   530   528   526   524   522

(a) Oxygen 1s binding energy.

Fe_{2p} 1/2 Fe_{2p} 3/2

0.001 N NaOH

.01 N NaOH

20 N NaOH

740   735   730   725   720   715   710   705   700

(b) Iron 2p 3/2 binding energy – 740 to 700 eV.

Fe_{2p} 3/2

0.001 N NaOH

.01 N NaOH

20 N NaOH

716   714   712   710   708   706   704   702

(c) Iron 2p 3/2 binding energy – 716 to 702 eV.

Na

1082   1080   1078   1076   1074   1072   1070   1068

Binding energy, eV

(d) Sodium binding energy.

Figure 21. – XPS data indicating effect of sodium hydroxide normality on wear surface chemistry.
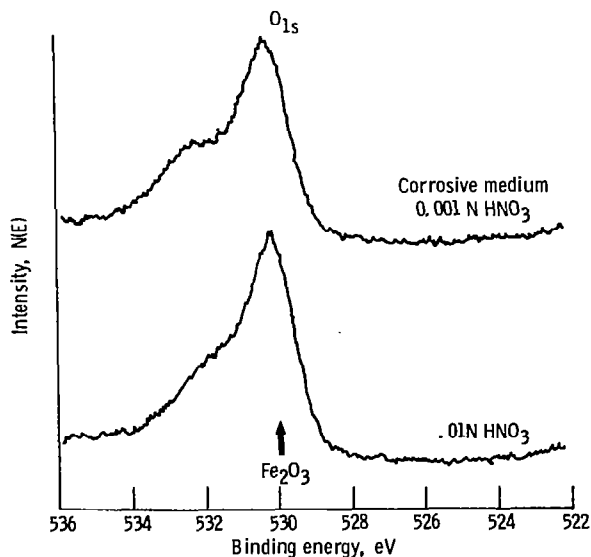
14

Figure 22. - XPS data indicating effect of nitric acid normality on wear surface chemistry.

1. With increasing concentrations of sodium hydroxide (NaOH) beyond 0.01 N, the friction and wear to the iron surface decrease. This decrease is accompanied by a decrease in the surface concentration of ferric oxide (Fe_2O_3) and in the width of the wear track.

2. Increasing concentrations of nitric acid (HNO_3) to 0.05 N results in a decrease in friction coefficient, but further increasing the concentration to 1.0 N causes no further change in friction behavior. Just as with NaOH, the decrease in friction is accompanied by a decrease in wear track width. Unlike with NaOH, however, the concentration of Fe_2O_3 increases with increasing normality of HNO_3.

3. The friction behavior of iron in both sulfuric acid (H_2SO_4) and sodium chloride (NaCl) salt were relatively unchanged with changes in normality.

4. X-ray photoelectron spectroscopy (XPS) analysis indicates that the iron surface contains both sulfates of iron as well as oxides when exposed under rubbing conditions to H_2SO_4.

5. XPS analysis indicates that the iron surface contains iron chlorides but no sodium in the surface films when exposed under rubbing conditions to NaCl.

Lewis Research Center,
National Aeronautics and Space Administration
Cleveland, Ohio, February 24, 1981.

References

1. Eyre, T. S.: Wear Characteristics of Metals. Source Book on Wear Control Technology, D. A. Rigney and W. A. Glaeser, eds., American Society for Metals, 1978, pp. 1-10. (Originally in Tribol. Int., vol. 9, no. 5, Oct. 1976, pp, 203-212.)
2. Neale, M. J., ed.: Tribology Handbook. Butterworths (London), 1973 (Section on Lubricants).
3. Waterhouse, R. B.: Fretting in Hostile Environments. Source Book on Wear Control Technology, D. A. Rigney and W. A. Glaeser, eds., American Society for Metals, 1978, pp. 261-269. Originally presented at the 3rd International Tribology Conference, Tribology for the Eighties, Paisley, Scotland, Sept. 22-25, 1975. (Also Wear, vol. 34, 1975, pp. 301-309.)
4. Bowden, F. P.; and Tabor, D.: The Friction and Lubrication of Solids. Oxford University Press (London), 1950 (with corrections through 1971).
5. Rabinowicz, E.: Fricton and Wear of Materials. John Wiley & Sons, Inc., 1965.
6. Staehle, R. W.: Stress Corrosion Cracking (and Corrosion Fatigue). Mater. Sci. Eng., vol. 25, Sept.-Oct. 1976, pp. 207-215.
7. Fontana, M. G.; and Greene, N. D.: Corrosion Engineering, 2nd ed. McGraw-Hill Book Co., Inc., 1978.
8. Logan, H. L.: The Stress Corrosion of Metals. John Wiley & Sons, Inc., 1966.
9. Brown, B. F.: A Preface to the Problem of Stress Corrosion Cracking. Stress Corrosion Cracking of Metals — A State of the Art, ASTM STP-518, American Society for Testing Materials, 1972, pp. 3-15.
10. Miyoshi, Kasuhisa; and Buckley, Donald H.: Surface Chemistry and Friction Behavior of Silicon Carbide (0001) Surface at Temperatures to 1500° C. NASA TP-1813, 1981.

1. Report No. NASA TP-1985	2. Government Accession No.	3. Recipient's Catalog No.
4. Title and Subtitle FRICTION AND WEAR OF IRON IN CORROSIVE MEDIA		5. Report Date March 1982
		6. Performing Organization Code 506-53-12
7. Author(s) George W. P. Rengstorff, Kazuhisa Miyoshi, and Donald H. Buckley		8. Performing Organization Report No. E-638
		10. Work Unit No.
9. Performing Organization Name and Address National Aeronautics and Space Administration Lewis Research Center Cleveland, Ohio 44135		11. Contract or Grant No.
		13. Type of Report and Period Covered Technical Paper
12. Sponsoring Agency Name and Address National Aeronautics and Space Administration Washington, D.C. 20546		14. Sponsoring Agency Code

15. Supplementary Notes

16. Abstract

Friction and wear experiments were conducted with elemental iron exposed to various corrosive media including two acids, a base, and a salt. Studies involved various concentrations of nitric and sulfuric acids, sodium hydroxide, and sodium chloride. Load and reciprocating sliding speed were kept constant. With the base NaOH an increase in normality beyond 0.01 N resulted in a decrease in both friction and wear. XPS analysis of the surface showed a decreasing concentration of ferric oxide (Fe_2O_3) on the iron surface with increasing NaOH concentration. With nitric acid (HNO_3) friction decreased in solutions to 0.05 N, beyond which no further change in friction was observed. The concentration of Fe_2O_3 on the surface continued to increase with increasing normality. XPS analysis revealed the presence of sulfates in addition to Fe_2O_3 on surfaces exposed to sulfuric acid (H_2SO_4) and iron chlorides but no sodium on surfaces exposed to NaCl.

17. Key Words (Suggested by Author(s)) Friction Wear Corrosive media	18. Distribution Statement Unclassified – unlimited STAR Category 26

19. Security Classif. (of this report) Unclassified	20. Security Classif. (of this page) Unclassified	21. No. of Pages 17	22. Price* A02